An Investigation into Impacting Techniques for Simulating Foreign Object Damage and Their Influence on the Fatigue Limit Strength of Ti-6Al-4V

Steven R. Thompson
United States Air Force Research Laboratory
Materials and Manufacturing Directorate
AFRL/MLSC
steven.thompson@wpafb.af.mil

Theodore Nicholas
United States Air Force Institute of Technology
AFIT/ENY

John J. Ruschau
William J. Porter
Dennis J. Buchanan
University of Dayton Research Institute

ABSTRACT

Foreign objects ingested into a gas turbine engine can cause a severe degradation of the fatigue properties of the impacted engine airfoils. Even small objects, such as sand, can cause damage that can reduce the fatigue capability of the material. Several factors have to be considered when evaluating the residual fatigue strength of an impacted material: a) the geometry of the impact damage such as the shape or stress concentration of a crater or dent, b) the role of residual stresses imparted to the material during the impact event, and c) the actual damage in terms of cracking or other microstructural damage. Ballistic impact was used as a baseline since it most closely represents an actual FOD event in an operating engine. To further understand the role of type of impact on the dynamic behavior of the material, other techniques were used to impart damage to the material. Specifically, quasi-static and low-speed pendulum impacts were used. Damage was imparted by these methods using the depth of the ballistic impacts as a reference. The baseline specimen used for this program was a diamond cross-section axial fatigue specimen with edges that were of similar geometry to the leading edge of a turbine engine airfoil. These leading edge specimens, machined from Ti-6Al-4V forged plate material in STOA condition, were fatigue tested in tension using a step-loading technique. Half of the specimens were stress relief annealed prior to testing (post-impact) to eliminate residual stresses.

Attempts have been made in this research effort to sort out the role of the individual factors leading to a fatigue debit, however the variability in damage from ballistic impacts of small hard particles on airfoil leading edge geometries have tended to obscure any specific conclusions on the role of each mechanism. A further investigation consisted of a comprehensive series of experiments under very controlled conditions. Ballistic impacts were made normal to the surface of flat plates. The plate specimens, of the same material used in the leading edge impacts, were then fatigue tested in tension, bending, and torsion (shear) using the step-loading technique. As with the airfoil specimens, half of the specimens were stress relief annealed in order to eliminate any residual stresses and to be able to sort out the effects of residual stresses on the fatigue limit strength. Because of the simple impact geometry of a flat plate impacted normally, as opposed to impacting a leading edge at a non-zero angle of incidence, the scatter in material behavior was reduced

Thompson, S.R.; Nicholas, T.; Ruschau, J.J.; Porter, W.J.; Buchanan, D.J. (2005) An Investigation into Impacting Techniques for Simulating Foreign Object Damage and Their Influence on the Fatigue Limit Strength of Ti-6Al-4V. In *Evaluation, Control and Prevention of High Cycle Fatigue in Gas Turbine Engines for Land, Sea and Air Vehicles* (pp. 13-1 – 13-18). Meeting Proceedings RTO-MP-AVT-121, Paper 13. Neuilly-sur-Seine, France: RTO. Available from: http://www.rto.nato.int/abstracts.asp.

Report Documentation Page

Form Approved
OMB No. 0704-0188

1. REPORT DATE	2. REPORT TYPE	3. DATES COVERED
01 OCT 2005	**N/A**	**-**

4. TITLE AND SUBTITLE	5a. CONTRACT NUMBER
An Investigation into Impacting Techniques for Simulating Foreign Object Damage and Their Influence on the Fatigue Limit Strength of Ti-6Al-4V	5b. GRANT NUMBER
	5c. PROGRAM ELEMENT NUMBER
6. AUTHOR(S)	5d. PROJECT NUMBER
	5e. TASK NUMBER
	5f. WORK UNIT NUMBER
7. PERFORMING ORGANIZATION NAME(S) AND ADDRESS(ES) **United States Air Force Research Laboratory Materials and Manufacturing Directorate AFRL/MLSC**	8. PERFORMING ORGANIZATION REPORT NUMBER
9. SPONSORING/MONITORING AGENCY NAME(S) AND ADDRESS(ES)	10. SPONSOR/MONITOR'S ACRONYM(S)
	11. SPONSOR/MONITOR'S REPORT NUMBER(S)

12. DISTRIBUTION/AVAILABILITY STATEMENT
Approved for public release, distribution unlimited

13. SUPPLEMENTARY NOTES
See also ADM202115, RTO-MP-AVT-121. Evaluation, Control and Prevention of High Cycle Fatigue in Gas Turbine Engines for Land, Sea and Air Vehicles., The original document contains color images.

14. ABSTRACT

15. SUBJECT TERMS

16. SECURITY CLASSIFICATION OF:			17. LIMITATION OF ABSTRACT	18. NUMBER OF PAGES	19a. NAME OF RESPONSIBLE PERSON
a. REPORT	b. ABSTRACT	c. THIS PAGE			
unclassified	**unclassified**	**unclassified**	**UU**	**18**	

somewhat.

Elastic stress concentration factors, k_t, were computed using a FEM simulation of both the damaged leading-edge and indented flat plate geometries. Experimental values of the fatigue notch factor, k_f, and k_t were compared for the different methods of imparting damage as well as for the different loading conditions. For the flat plate specimens, fractography was conducted on selected samples to locate the fatigue origin and to relate this to k_t at a given location, taking into account the residual stresses imparted during any of the impact or indent procedures. This large body of data has been sorted to try to quantify and explain the relative contributions of the critical parameters involved in FOD.

.

1.0 INTRODUCTION

High cycle fatigue (HCF) failures in military gas turbine engines is typically caused by a combination of high frequency vibratory stresses and in-service damage incurred by events such as foreign object damage (FOD), fretting, and low-cycle fatigue. FOD is caused by particles such as sand or runway debris being ingested into the engine and the subsequent impacting of these particles against components typically in the fan and compressor regions. The issues dealing with FOD have been summarized previously, but it is not an overstatement to say that even the smallest FOD damage can have a detrimental effect on the structural integrity of rotating components in the engine [1].

The damage incurred during a FOD event will typically consist of a notch-like feature in the component that can reduce the material's fatigue strength. This degradation can be attributed to three primary factors: a stress concentration due to the geometry of the damage, tensile residual stresses developed around the damage site, and physical damage [2,3]. On the beneficial side, compressive residual stresses and strain hardening can improve the baseline fatigue properties. Of the factors affecting the fatigue strength, the stress concentration is easiest to handle by using theoretical or empirical notch fatigue factors applied to measured notch profiles. Many times, the geometry of the notch is simulated in the laboratory using simple indentation methods as opposed to a more realistic ballistic impact. Analyses resulting from this type of procedure can raise questions if the damage produced differs from the real event even though the notch geometry produced is identical [4].

Determining the role that residual stresses play in affecting fatigue strength has been handled in this and previous investigations through the use of stress relief annealing of a portion of the titanium specimens [5,6]. By careful annealing, residual stresses are effectively eliminated while preserving the microstructural and mechanical characteristics of the material.

The greatest challenge, however, is in characterizing the role of the actual physical damage on the fatigue strength. An additional challenge is to relate the extent of the microstructural damage and the geometrical features to the characteristics of the impacting object including velocity and impact energy. In this investigation, damage induced by FOD in a leading edge geometry representative of a fan blade is quantified through a series of experiments involving variations of impact velocity and size of impactors. Comparisons are made of the methods of inducing damage which range in speed from quasi-static to ballistic while producing damage which is nearly identical from a geometry viewpoint.

2.0 EXPERIMENTAL PROCEDURES

The test material was Ti-6Al-4V forged plate approximately 20 mm thick that had been heat-treated to the STOA condition. The result was an alpha-beta titanium alloy microstructure with acicular Widmanstätten structures. It is identical to the material used in prior investigations in several laboratories as part of the National Turbine Engine High Cycle Fatigue Program [1,2,4-7].

2.1 Airfoil Specimens

The simulated airfoil specimen configuration is a diamond cross-section tension specimen. The specimen was designed such that the edges of the gage section are tapered at an angle and to a radius representative of the leading edge on a typical fan blade. The samples were ballistically impacted on each leading edge (2 per sample) using a single-stage compressed gas gun. Details of the specimen and the ballistic impact procedures have been described previously in [7]. The samples were shot with steel spheres of nominal diameters of 0.5, 1.33, and 2.0 mm at velocities ranging from approximately 40 to 520 m/s at an angle of 30°, relative to a head-on impact to the tapered edge. Several combinations of impact conditions were selected to obtain similar kinetic energy levels from different size projectiles.

Quasi-static indentation was accomplished using a servo-electric testing machine under displacement control to produce notches that were geometrically similar to those obtained via ballistic impact. This was accomplished using steel indentors that had the same radii as the ballistically impacting spheres and accounting for elasticity (rebound) of the specimen and supporting fixture. These same indentors were also fitted onto a pendulum as a third method of imparting damage. Pendulum mass and velocity conditions were chosen to produce similar values of depth of penetration to those of the sphere impacts and quasi-static indents, typically in the range of 0.18 – 0.75 mm.

To establish the fatigue strength, samples were fatigue tested using the step-loading procedures described by Maxwell and Nicholas [8], which allows obtaining a fatigue limit stress using a single specimen with no load history effects. Steps of 10^7 cycles were used in this investigation with $\Delta\sigma$ set at 10% of the initial load block. Testing was conducted at a stress ratio (R) of 0.1 and a frequency of 350 Hz using an electro-dynamic, shaker-based test machine. All testing was performed in ambient laboratory air conditions. Further details of the experimental procedures can be found in [1,3,5,6,7].

2.2 Flat Plate Specimens

For the ballistic impacts, steel spheres, 3.18 mm in diameter, were impacted normally at velocities of either 200 or 300 m/s onto 3.18 mm thick flat plates of the same Ti-6Al-4V forged plate material. Half of the specimens were stress relief (SR) annealed at 704°C for 1 hr in order to eliminate any residual stresses and to ascertain the effects of residual stresses on the fatigue limit strength. To compare ballistic impact damage to typical laboratory simulations, damage was imparted to the material in the form of either a quasi-static ball indentation or the low velocity impact of a ball using a pendulum to the identical depths as obtained in the ballistic experiments. In both types of impacts, the ball used for producing the indent was the same diameter and material as that used in the ballistic impacts. The depth of indent for the quasi-static and pendulum indents was chosen to be the same as the average value for the ballistic impacts, 0.22 and 0.41 mm, for the 200 and 300 m/s impacts, respectively. As in the case of the ballistic impacts, stress relief annealing was used on half of the quasi-static and pendulum impact specimens. All of the plate specimens were then fatigue tested in tension or torsion using a step-loading technique [8] to determine the fatigue limit stress, σ_{FLS}, corresponding to a life of 10^6 cycles. The choice of 10^6 cycles was made for convenience only in order to minimize testing

time. In reality, more than 10^7 cycles would represent real high cycle fatigue behavior. The torsion tests were added to tensile testing on the flat plate samples in order to produce different failure locations where residual stresses might be different.

3.0 RESULTS AND DISCUSSION

3.1 Airfoil Specimens

3.1.1 Analysis

The reduction of fatigue strength due to a notch is commonly characterized by a fatigue notch factor, k_f, which is defined as the ratio of the smooth bar fatigue strength to that of the notched bar based on net cross sectional area,

$$k_f = \frac{\sigma_{smooth}}{\sigma_{notched}}. \quad (1)$$

The value of k_f can be predicted from the elastic stress concentration factor, k_t, through empirical formulae that fit experimental data. In this investigation, the notch is assumed to have a radius equal to the impacting sphere or the static indentor, an assumption that was verified in prior investigations on the same material [3,5,6]. Finite element analyses of ideal 30° notches were used to determine k_t for several different combinations of radii and depths. The values of k_f chosen for this investigation are those given by Peterson [9] in the form,

$$k_f = 1 + \frac{(k_t - 1)}{(1 + a_p / r)} \quad (2)$$

using a_p = 300 μm as a material constant obtained from fitting notch fatigue data in a previous study [10] on the same material and where r is the radius of the notch.

3.1.2 Test Results

The results for the fatigue limit stress, normalized with respect to the smooth bar fatigue strength at R=0.1, 10^7 cycles (568 MPa), are presented in Fig. 1 as a function of the measured notch depth. Most of the data in this investigation were obtained for impacts with a ball diameter of 1.33 mm and quasi-static and pendulum indents with the same diameter chisel. Shown also is a reference line corresponding to the fatigue notch factor as calculated for a notch radius of 0.67 mm from Eq. 2. In the nomenclature used, hollow symbols refer to stress-relieved (SR) specimens, whereas solid symbols are for specimens tested as-received (AR) after impacting or indenting. Data obtained at three different ballistic velocities (having significantly different kinetic energies) are noted, as well as results for the quasi-static and pendulum indents of similar impact depths.

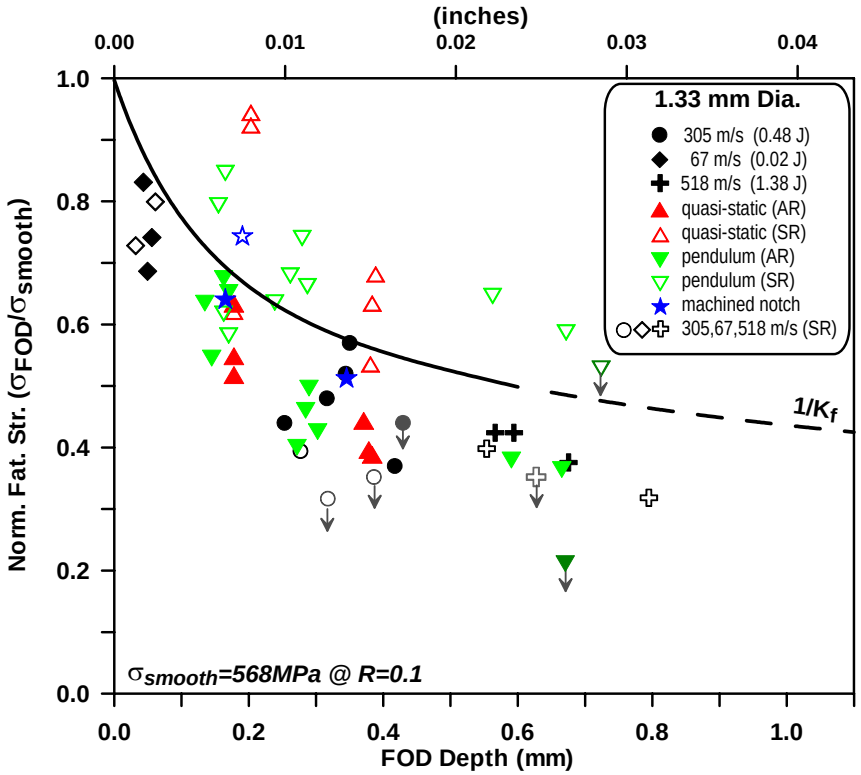

Figure 1. Normalized fatigue strength as a function of FOD depth for 1.33 mm dia. indents.

A prediction, based solely on notch geometry using k_f is also shown in the figure. (Since the fatigue strength is normalized, the prediction appears as a line calculated as $1/k_f$.) It should be noted that this line does not take into consideration any microstructural damage imparted by the impacts or any residual stresses produced during the impacts. The data of the as-impacted (AR) specimens follow essentially the same trend, which is slightly lower than the prediction regardless of the impacting technique. By comparison, the fatigue strength of specimens with machined notches of depths of approximately 0.2 and 0.4 mm were only slightly lower that as predicted by the k_f formula. A single specimen with a machined notch of approximately 0.2 mm was stress-relieved and tested and had a slightly higher fatigue strength than the prediction by the k_f formula. Although careful low-stress grinding procedures were used, these specimens show that even small amounts of residual stress can effect the resultant fatigue strength. Since the predicted strength appears to be equidistant between the as-received and stress relieved machined notch results, the validity of the k_f formulation for these notch geometries was believed to be confirmed.

The hollow triangles in Fig. 1 show the effect of removing residual stress effects from the quasi-static and pendulum indents, which indicates that the fatigue strength increases due to stress relief. This would imply that the indenting procedures imparted tensile residual stresses. The apparent strengthening effect over that predicted by k_f analysis can be partially explained by observing the geometry of the non-ballistic notch after indentation as compared to a machined notch, as shown in Fig. 2. The indent produced by quasi-static methods produces substantial bulging, plastic deformation, and distortion of the notch, as shown in Fig. 2b.

The net effect invalidates the k_t approximation used because of the distorted geometry. Nonetheless, the increase in the fatigue strength over the as-impacted results clearly demonstrates the role of tensile residual stresses, when using the quasi-static methods.

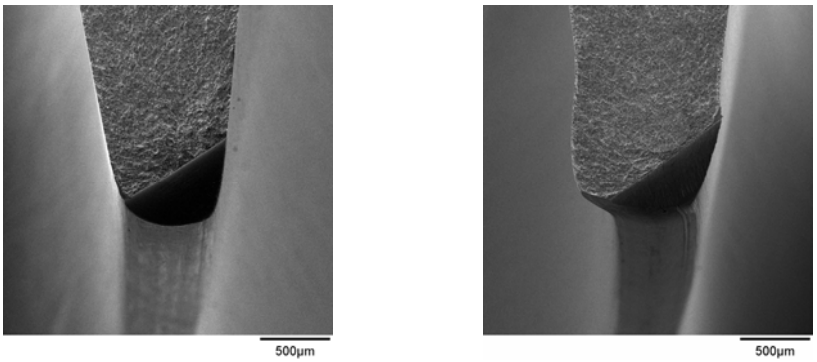

(a) (b)

Figure 2. Comparison of (a) machined notch and (b) quasi-static indent profiles.

Another possible contribution to the apparent strengthening effect on the SR samples is the strain hardening that takes place during the deformation process when the crater is formed. Both the quasi-static and pendulum impacts show an apparent strengthening effect when stress relieved, but the net effect produces fatigue strengths above that predicted solely by the geometry. In addition to the difference in deformation pattern discussed above, it is thought that some strengthening in fatigue from strain hardening in compression may have occurred.

Stress relief of the specimens that were ballistically impacted, on the other hand, produced little or no change in fatigue strength as shown by the hollow circles and crosses in Fig. 1. Here it would appear that the ballistic impacting produces minimal residual stresses and perhaps beneficial compressive stresses dominate. (A downward arrow in a data point indicates that it failed during the first loading block of the step test procedure.) This observation of apparent compressive residual stresses is consistent with observations from numerical simulations of spherical ball impacts on this leading edge geometry, which show tendencies for compressive stresses to develop near the exit side of the crater for an ideal impact [11].

Data for the impacts with the 2.0 mm diameter spheres/indentor is shown in Fig. 3. (The results for the specimens that were impacted with the 0.5 diameter spheres, as well as an analysis into the energy levels used to impart the damage for all of the specimens are described in Ref [7].) For these spheres causing the deepest notches, the formula corresponding to k_f tends to over predict the fatigue limit stresses, particularly when the notch depth approaches 1 mm. Here, for the ballistic impacts, the stress relief procedure has little or no effect on the fatigue strength, indicating the absence of significant residual stresses in the vicinity of the damage site. The quasi-static indented specimens, on the other hand, exhibit the same type of behavior as seen in the 1.33 mm diameter specimens described above. Again, this may be attributed to some combination of the deformation pattern observed (Fig. 2) and possible strain hardening effects.

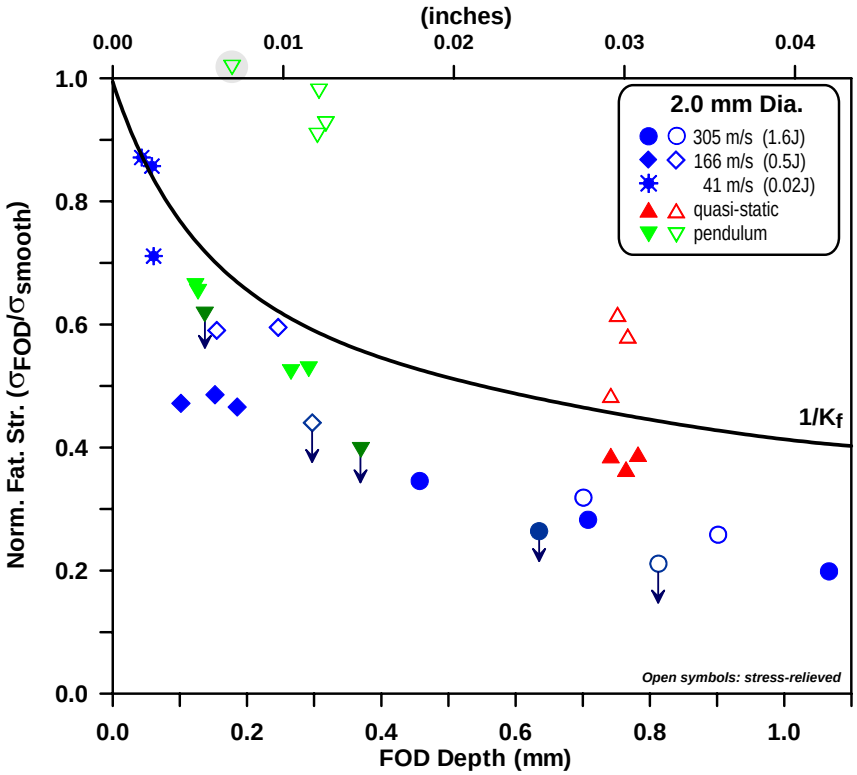

Figure 3. Normalized fatigue strength as a function of FOD depth for 2.0 mm dia. indents.

One reason for the lower strength of specimens with ballistic damage after stress relief is attributable to the physical appearance of the damage sites. For the impacts with the larger ballistic damage sites, most of the leading edge specimens were chipped or fractured and exhibited what has been termed loss of material (LOM) [3,5], as seen in the SEM photo, Fig. 4(a). Some of the specimen impacts had only permanent deformation (dents) as seen in the SEM photo in Fig 4(b). The depth of penetration of all of the impacts can be correlated well with impact energy, as would be expected, except for cases where fracture occurred locally. In that case, the depth of penetration is generally higher and represents the worst-case scenario regarding fatigue strength debit as noted also in previous research [3,5]. Of particular interest here also is that for the quasi-static indents, there were no instances where LOM occurred, even for the largest imparted energy cases examined. Preliminary examinations of deep pendulum indents show large amounts of deformation and possible cracking.

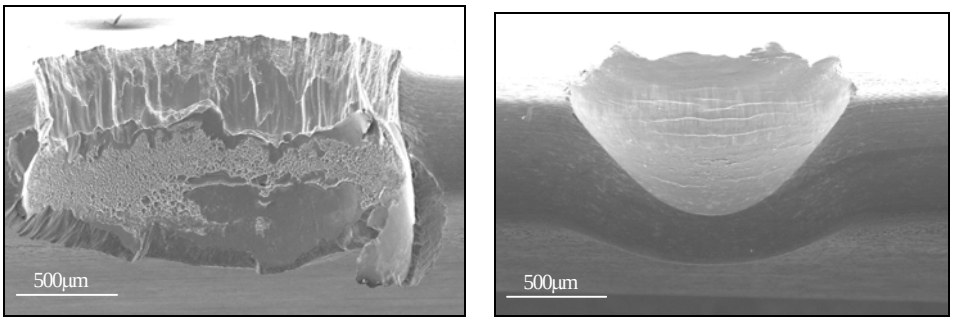

(a) LOM (b) Dented

Figure 4. SEM photos of indents showing (a) loss of material and (b) indentation

A general observation that can be made of all the data is that residual stresses that are produced by ballistic impact depend on the size and velocity of the impacting sphere. These stresses may be different in magnitude and type (tension vs. compression) depending on their appearance when going from ballistic impacts to quasi-static indentation. Further, it has been observed in numerical simulations that the residual stresses are extremely sensitive to the exact location of the impact on a leading edge geometry [11]. Perhaps the most significant observation is that the fatigue limit stress of a ballistically impacted leading edge specimen can be reduced by as much as 70-80 percent in the specimens that had the largest amount of damage. While these were the most severe impact conditions in these experiments, these are still rather small impacting objects compared to stones, tools, and even some sand particles that have caused FOD in gas turbine engines in both military and civilian aircraft.

3.2 Flat Plate Specimens

3.2.1 Analysis

The stress distribution and an effective elastic stress concentration factor were determined for the two notch geometries from a finite element simulation of the rectangular test specimens. The depth of indent for the notch geometry was 0.22 and 0.41 mm for the shallow and deep notches, respectively. It was assumed throughout that the notch has a spherical surface with a radius of one-half of the impacting sphere whose diameter was 3.18 mm. The finite element model for calculating the stress distribution used the geometry and coordinate system shown in Fig. 5 for half the cross section through the middle of the notch. The rectangular specimens were 3.18 mm thick and 10.0 mm wide. The entire specimen was modeled in the FEM analysis. Calculations were carried out for a specimen subjected to tension, bending about the weak axis, or torsion, but for this investigation only tension and torsion experiments were conducted. The commercial finite element code, ANSYS, was employed for all analyses. Twenty-node solid brick elements were selected to accurately model the spherical surface. These higher-order elements are more appropriate for capturing the stress gradients at the notch. Mesh refinement in the vicinity of the notch was performed to determine the accuracy of the stress concentration factor. Final element size in the vicinity of the notch was approximately 0.020 mm.

The analytical results for the maximum tensile stresses due to an average axial stress of 100 MPa, a bending moment that causes 100 MPa along the surface, or a torque that produces 100 MPa at the surface are presented in Fig. 6 as a function of the y-axis location as denoted in Fig. 5. (The ANSYS output is given along the surface coordinate, s). For the axial and bending cases, the maximum tensile stress is in the axial direction of the specimen. For the torsion case, the maximum tensile stresses are perpendicular to a plane inclined at 45° to the axial direction. In all cases, the stresses shown are for a plane that cuts through the center of the

notch. The center of the notch corresponds to y = 5 mm (10 mm wide plate) and the coordinates for the point A in Fig. 5, where the notch intersects the surface of the plate, are y = 4.201 and y = 3.939 mm for the shallow and deep notches, respectively. This location is shown as the edge of notch in Fig. 6 as a dotted line. For the torsion case, the maximum tension occurs on a plane inclined at an angle of 45° to the axis of the specimen. For this case, the stresses are computed along that inclined plane and the center of the notch is retained at a coordinate defined by y = 5 mm where the y-axis is also inclined at 45°. In this case, y = 0 is not at the edge of the plate.

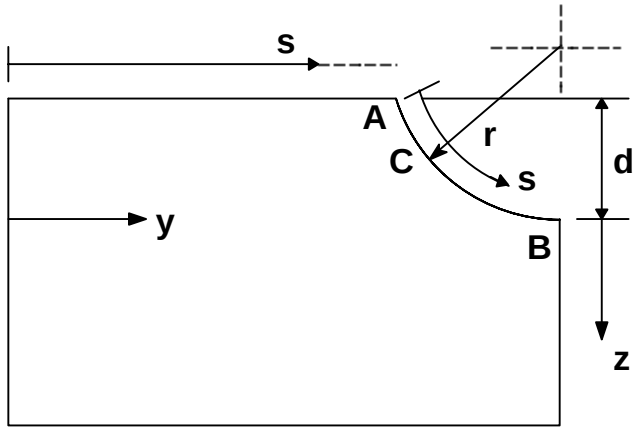

Figure 5. Geometry of half cross section through middle of notch for the Flat Plate Specimens.

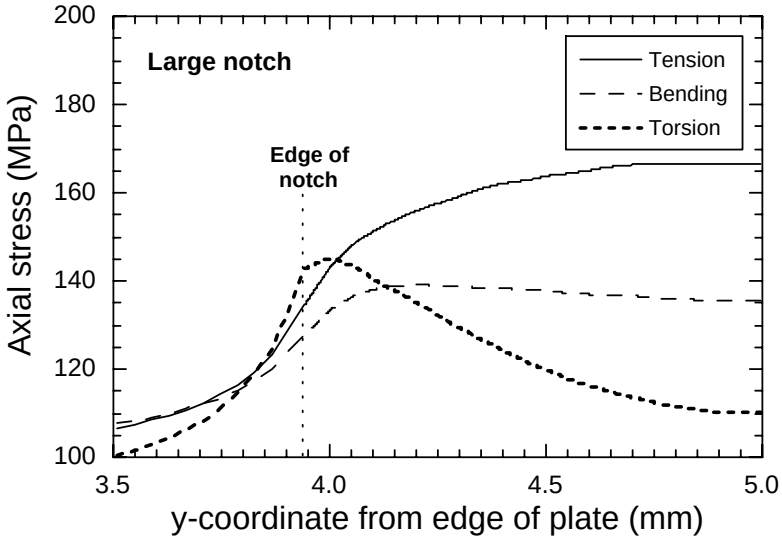

Figure 6. Maximum tensile stress distribution along surface of plate with large notch.

Values of k_t are summarized for the two notch sizes in Figs. 7 and 8. These computations are based on the true definition of a stress concentration factor: the actual stress at a location divided by the stress at that same location if the notch were not present. For axial loading, this is no problem since the smooth bar stresses are uniform across the cross section. However, for bending or torsion where the stresses in a smooth bar vary linearly through the cross section, the value of the smooth bar stress decreases from the surface towards the notch bottom. A better measure of the notch effect is to use an effective stress concentration factor, denoted by k_t', defined as the local stress in the notched specimen divided by the maximum stress at the surface in the smooth bar. The difference between the two quantities can be easily seen by comparing the true k_t for torsion in the large notch specimen, Fig. 8, with the actual stress distribution in Fig. 6. The value of k_t' is simply the value of the stress, such as shown in Fig. 6 for the large notch, divided by the reference far field stress, 100 MPa. Values for the effective stress concentration for the axial tension, pure bending, and torsion cases are summarized in Table 1. For most cases, the locations for the maximum value of the local stress concentration are either at A along the surface at the edge of the notch or at B at the root of the notch, the latter having the larger k_t in most cases for axial tension loading. However, for the deep (large) notch under bending or torsion and the small notch under bending, the maximum value of k_t' occurs at point C at the interior of the notch as seen in Fig. 6. It is slightly higher than the value at point B at the bottom of the notch for the bending case and slightly higher than at the surface, point A, for the torsion case.

Table 1. Computed values of k_t' for notches in Flat Plate Specimens.

	Small notch		Large notch	
	Bottom	Surface	Bottom	Surface
Axial	1.51	1.24	1.67	1.35
Bending	1.36	1.18	1.36	1.28, 1.39*
Torsion	1.13	1.26, 1.32**	1.10	1.38, 1.46***

*@ y = 4.20 mm, **@ y = 4.25 mm , ***@ y = 4.00 mm

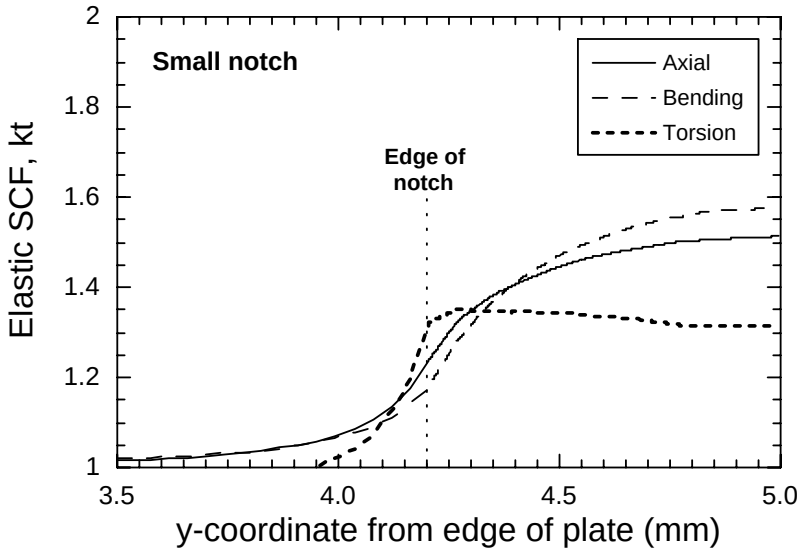

Figure 7. Elastic stress concentration factor along surface of small notch.

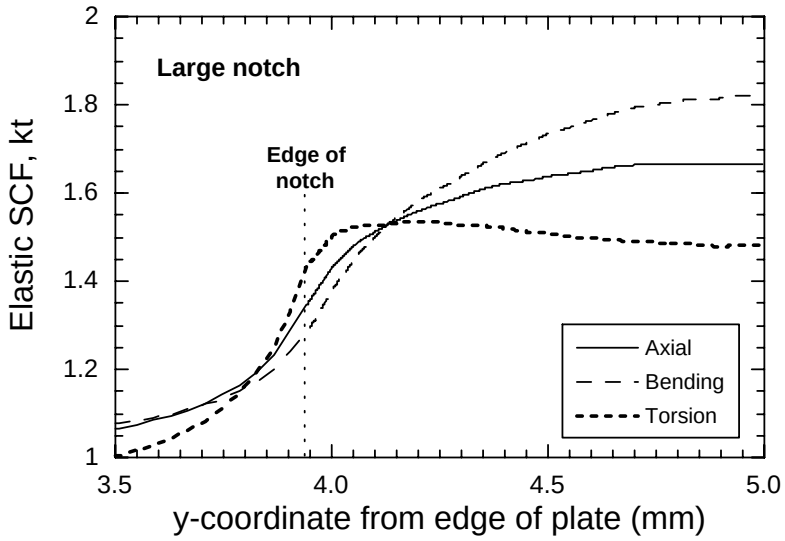

Figure 8. Elastic stress concentration factor along surface of large notch.

3.2.2 Test Results

The fatigue limit stress, σ_{FLS}, corresponding to a life of 10^6 cycles was determined from step tests [8] in both tension and torsion using the interpolation formula

$$\sigma_{FLS} = \sigma_{prior} + \Delta\sigma \left(\frac{N_f}{10^6} \right) \tag{3}$$

where σ_{prior} is the stress in the cycle block prior to failure, N_f is the number of cycles in the last block where failure occurs, and $\Delta\sigma$ is the stress increment going from the prior block to the last block. For each value of σ_{FLS}, the fatigue notch factor, k_f, was calculated from the definition, Eqn (1).

The value of σ_{FLS} for smooth bar tension tests on this material at 10^6 cycles was 600 MPa at R = 0.1. The results for the average value of k_f from at least 2 tests at each of the conditions shown are summarized in Table 2 for tension tests conducted at R = 0.1. In all cases, for both tension and torsion, the results of the max or min values were within 11% of the mean which is the data point presented. The symbol "AR" is used to denote as-received material, that is, material as tested without stress relief after the indents were put in. The symbol "SR" denotes samples that were stress relieved after indentation. Three types of indentations are represented in this data base. The pendulum impacts were conducted at the necessary velocities, around a few m/s, to obtain the targeted penetration depths with the mass of the impacting fixture. The results of all of the tensile fatigue tests show that stress relief (SR) improved the fatigue strength in all of the cases, although the improvement was not very large. This implies that some tensile residual stresses were present after all of the indentation procedures, since nothing changes during the SR process other than the removal of residual stresses. This finding is consistent with the results on the airfoil specimens. These results, however, are in conflict with computations of residual stresses under impact conditions where residual stresses are reported to be compressive at the bottom of the notch [12].

Table 2. Experimental values of k_f for notches under tension, R = 0.1.

Notch type	Ballistic	Pendulum	Quasi-static
AR Shallow	1.31	1.20	1.19
AR Deep	1.69	1.31	1.26
SR Shallow	1.26	1.10	1.07
SR Deep	1.53	1.11	1.09

Of greater significance in the findings here is the observation that ballistic impacts to the same depth as pendulum or quasi-static indentations are more severe in terms of the resulting fatigue limit strength or notch fatigue factor. This is especially true for the deeper indents corresponding to ballistic impacts at 300 m/s. In the work of Peters et al. [2], the impacts at 300 m/s produced small amounts of cracking at the crater whereas the impacts at 200 m/s produced no observable cracks. From these observations, it is concluded that low velocity (pendulum) or quasi-static indentation does not produce the same amount of damage as ballistic impact, particularly at higher velocities, even though the resulting craters are of the same dimension.

Results for the tests in torsion (average of at least two tests) are summarized in Table 3. Here, only

ballistic impacts were evaluated. The test matrix was limited to R = 0 for both AR and SR samples, and to R = -1 for AR only. The SR samples show a reduction in k_f which is equivalent to an increase in σ_{FLS}. This is attributed to the implied existence of tensile residual stresses at the location of failure initiation. The existence of tensile residual stresses is confirmed by the calculations of Chen and Hutchinson [12] who report tensile residual stresses at the crater surface from numerical simulations of impact of a ball on a half space.

Table 3. Experimental values of k_f for ballistic notches under torsion

Notch type	R = 0	R = -1
AR Shallow	1.31	1.62
AR Deep	2.00	2.00
SR Shallow	1.01	---
SR Deep	1.47	---

The value of k_t in Table 1 for a deep notch in tension indicates that fracture would be expected at the bottom of the notch. This is confirmed by the observed location of initiation near the notch bottom as shown in Fig. 9(a). On the other hand, torsion tests of a specimen with a shallow notch would be expected to produce a failure near the surface because of the higher value of k_t as listed in Table 1. The fractograph, Fig. 9(b), confirms such a finding. In both cases illustrated, the specimen was subjected to SR, so only microstructural damage or hardening could account for fracture initiating at any other location. The exception to this reasoning is illustrated in the fractograph, Fig. 10, where initiation is seen to occur near the surface of a deep notch from high velocity (312 m/s) ballistic impact. While initiation would be expected to occur at the bottom according to k_t analysis for tension fatigue loading, in this case damage was sufficient in the form of local tearing to reduce the fatigue strength below that of most of the other specimens. This resulted in fracture initiating near the location of extensive damage in the form of pile-up at the surface. Neither the damage or the alteration of the geometry are accounted for in the finite element analysis.

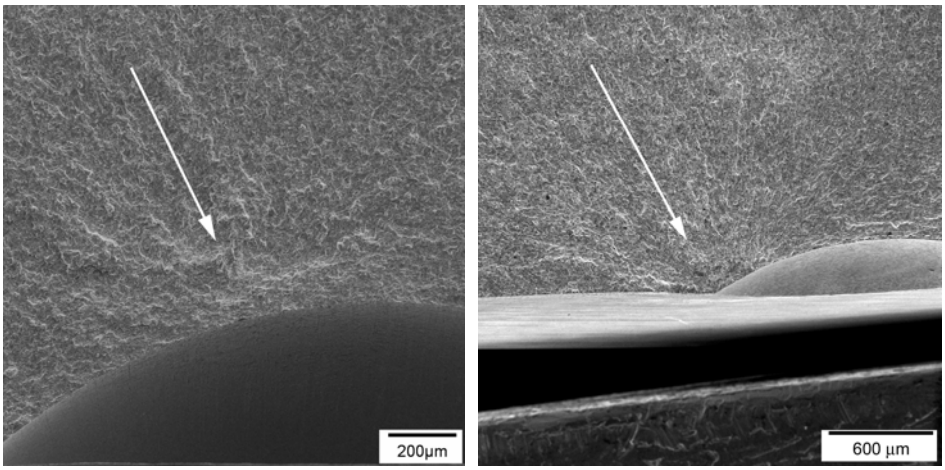

(a) (b)

Figure 9. Fractographs showing initiation sites in (a) tension, (b) torsion.

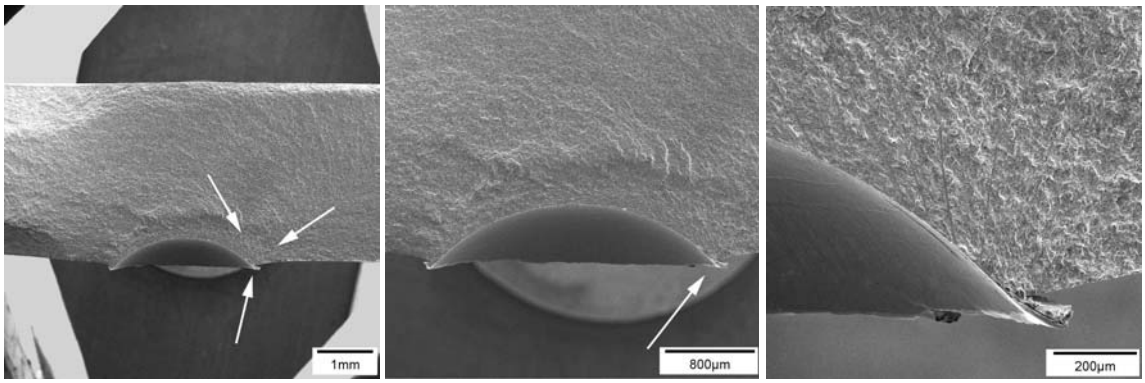

Figure 10. Fracture surface of torsion specimen showing initiation site near notch surface.

The difference in σ_{FLS} between AR and SR in the tension and torsion cases for ballistic impact seems to indicate that the tensile residual stresses are somewhat higher near the surface than at the bottom although scatter in test results makes this observation somewhat tenuous. In both the tension and torsion cases, for ballistic impact at 300 m/s which produces the deeper crater, the debit in fatigue strength is greater than that expected due solely to the stress concentration factor, indicating some type of microstructural damage near the failure location whether it be at the bottom, for tension tests, or near the surface, for torsion tests. Finally, for the shallow indents produced by ballistic impact at 200 m/s, there is no apparent reduction in fatigue strength under torsion testing after SR, even though the value of k_t is 1.32 at the failure location. This implies that some type of strengthening mechanism is present that retards fatigue failure, most likely delaying fatigue initiation. In a study of deep rolling and other surface treatments in this same alloy, Nalla et al. [13] identified a strengthening mechanism in the form of an induced work hardening near-surface layer that improves the

fatigue resistance of the material.

All of the data obtained in tension at R = 0.1 and torsion at R = 0 are summarized in Fig. 11 where hollow symbols represent the SR specimens and solid symbols are for specimens that were not stress relieved and are designated AR. This figure illustrates the trend of SR specimens to have higher strengths than AR specimens, even higher than would be expected from a k_t analysis. For reference purposes, the line representing $1/k_t$ is shown. Ideally, a line showing theoretical values of $1/k_f$, which would be somewhat higher, should be shown. However, for the notch geometry and loading conditions used here, there is no model for values of k_f.

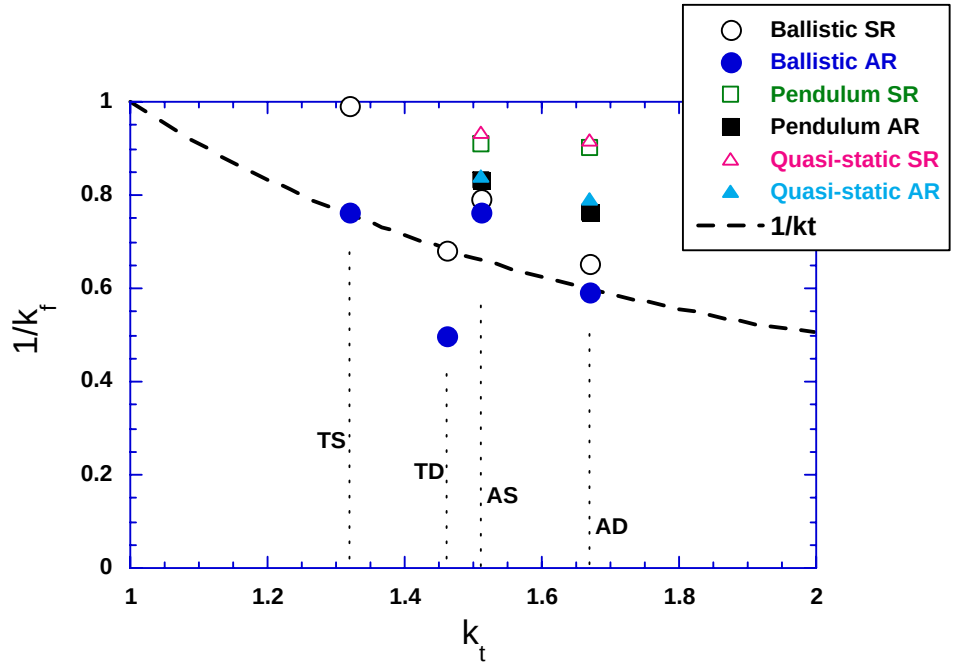

Figure 11. Fatigue limit strength for all tension (R = 0.1) and torsion (R = 0) tests. (A = axial, T = torsion, S = shallow notch, D = deep notch)

Figure 11 shows that the ballistic impacted specimens show degradation in strength beyond that predicted simply by k_t. The results are in agreement with those of Fig. 3 for airfoil leading edge samples tested in tension and imply both a tensile residual stress after impact as well as greater damage under ballistic impact than from quasi-static or pendulum indents. Additionally, the findings here are show other similarities to those on the airfoil specimens. As shown in Fig. 3, airfoil specimens subjected to quasi-static or pendulum impacts that are stress relieved generally show higher fatigue limit strengths than predicted by simple k_f formulas that are accurate for machined notches in the same geometry specimens.

4.0 SUMMARY AND CONCLUSIONS

The fatigue limit strength of a ballistically impacted leading edge specimen is influenced by not only the geometry of the notch produced by the impact, but by the residual stress field and mechanisms producing the notch. For notches with lesser amounts of damage, the impact site was predominately plastic deformation that resulted in a notch fatigue strength that is reasonably predicted by conventional notch analysis using k_f. Some strengthening effect, observed after stress relief annealing, can be attributed to possible strain hardening. Residual stresses, which tend to alter these strengths somewhat, are very sensitive to the nature of the impact and can be either tensile or compressive and very hard to predict. For larger ballistic damage levels, the notch crater exhibited damage such as chipping, local failure, and loss of material. In these cases, the fatigue strength was degraded compared to that predicted by k_f analysis and the energy absorbed was lower than for a similar geometry notch caused by plastic deformation. The fatigue strength is degraded the most when loss of material occurs. Quasi-static indenting used to produce craters of the same depth as the ballistic impacts resulted in plastic deformation in all the cases investigated. Smaller pendulum indents exhibit plastic deformation, while preliminary examinations of larger pendulum indents show the potential for greater physical damage. While a large LOM is not expected in these cases, it is anticipated that a condition can be found that will provide local fracture of material or small cracking, which should be enough to simulate the ballistic impact cases where LOM occurred. The types of FOD simulations where only plastic deformation occurs can slightly over-predict the fatigue strength for the same depth of penetration when compared to the ballistic case where loss of material occurs. While some of the quasi-static and pendulum impacts produced fatigue strengths that were similar to those from ballistic impacts of the same depths, the mechanisms producing the altered strengths are not always the same in the ballistic case compared to the simulated indents at much lower velocities.

Normal impacts on flat plates under ballistic and slower velocity conditions that produce craters of a given depth produce damage involving a number of mechanisms. The fatigue strength, that is a reflection of the damage severity, is also a function of loading conditions under axial or torsion stress states. Residual stresses are found to be tensile in most cases while some type of strengthening mechanism from the indenting exists that is not removed by stress relief annealing. For the deeper of the impacts encountered here, the impact damage from ballistic or lower velocity conditions reduces the fatigue strength beyond that predicted from the geometry of the resultant crater as characterized by the elastic stress concentration factor. Quasi-static and low velocity pendulum indents produce different damage mechanisms than equivalent depth craters from ballistic impacts even though the fatigue strengths may be similar.

5.0 ACKNOWLEDGEMENTS

The authors wish to acknowledge the support of Mssrs. Donald Woleslagle, David Maxwell, and Ken Goecke of the University of Dayton Research Institute (UDRI) for their substantial contributions to this research; and to Nick Jacobs (UDRI), John Stalter (UDRI) and David Iddings (Wright State University) for their efforts in the quasi-static and pendulum indentation of test specimens. Ballistic impacting was conducted at the Impact Physics Laboratory of UDRI.

6.0 REFERENCES

[1] Ruschau, J.J., Nicholas, T. and Thompson, S.R., "Influence of Foreign Object Damage (FOD) on Fatigue Life of Simulated Ti-6Al-4V Airfoils," Int. Jour. Impact Engineering, **25**, 2001, pp. 233-250.

[2] Peters, J.O., Roder, O., Boyce, B.L., Thomson, A.W. and Ritchie, R.O., "Role of Foreign Object Damage on Thresholds for High-Cycle Fatigue in Ti-6Al-4V," Metallurgical and Materials

Transactions A, Vol. 31A, June 2000, pp. 1571-1583.

[3] Birkbeck, J.C., "Effects of FOD on the Fatigue Crack Initiation of Ballistically Impacted Ti-6Al-4V Simulated Engine Blades," Ph.D. Thesis, School of Engineering, University of Dayton, Dayton, OH, August, 2002.

[4] Mall, S., Hamrick, J.L., II and Nicholas, T., "High Cycle Fatigue Behavior of Ti-6Al-4V with Simulated Foreign Object Damage," Mech. of Mat., **33**, 2001, pp. 679-692.

[5] Martinez, C.M., Birkbeck, J., Eylon, D., Nicholas, T., Thompson, S.R., Ruschau, J.J., and Porter, W.J., "Effects of Ballistic Impact Damage on Fatigue Crack Initiation in Ti-6Al-4V Simulated Engine Blades," Mat. Sci. Eng., **A325**, 2002, pp. 465-477.

[6] Thompson, S.R., Ruschau, J.J. and Nicholas, T., "Influence of Residual Stresses on High Cycle Fatigue Strength of Ti-6Al-4V Leading Edges Subjected to Foreign Object Damage," Int. J. Fatigue, **23**, 2001, pp. S405-S412.

[7] Ruschau, J.J., Thompson, S.R., and Nicholas, T., "High Cycle Fatigue Limit Stresses for Airfoils Subjected to Foreign Object Damage," Int. J. Fatigue, **25**, 2003, pp. 955-962.

[8] Maxwell, D.C. and Nicholas, T., "A Rapid Method for Generation of a Haigh Diagram For High Cycle Fatigue", in Fatigue and Fracture Mechanics: 29th Volume, STP 1321, T.L. Panontin and S.D. Sheppard (Eds.), American Society for Testing Materials, West Conshohocken, PA, 1999, pp. 626-641.

[9] Peterson, R. E., 1959, "Notch-Sensitivity," Metal Fatigue, G. Sines and J.L. Waisman, eds., McGraw-Hill, New York, pp. 293-306.

[10] Lanning, D.B., Nicholas, T. and Haritos, G.K., "On the Use of Critical Distance Theories for the Prediction of the High Cycle Fatigue Limit in Notched Ti-6Al-4V," Int. J. Fatigue, **27**, 2005, pp. 45-57.

[11] Bastnagel, P. et al., AADC, Indianapolis, IN, 2002, unpublished data.

[12] Chen, X. and Hutchinson, J.W., "Particle Impact on Metal Substrates with Application to Foreign Object Damage to Aircraft Engines," Jour. Mech. Phys. Solids., **50**, 2002, pp. 2669-2690.

[13] Nalla, R.K., Altenberger, I., Noster, U., Liu, G.Y., Scholtes, B. and Ritchie, R.O., "On the Influence of Mechanical Surface Treatments - Deep Rolling and Laser Shock Peening - on the Fatigue Behavior of Ti-6Al-4V at Ambient and Elevated Temperatures," Mat. Sci. Eng., **A355**, 2003, pp. 216-230.

SYMPOSIA DISCUSSION – PAPER NO: 13

Author's name: S. Thompson

Discussor's name: J. Schofield

Question: Why has a sphere been used in the tests? Why is an impact of 30° used on the airfoil specimens?

Answer: The sphere was used due to availability. It was also compatible with an earlier investigation that used glass spheres to simulate a sand ingestion FOD event.
The 30° impact angle was chosen based on input from engine manufacturers and simulates an angle that might occur from a particle moving against a rotating blade. In-house testing confirmed 30° as a worst-case angle.

Discussor's name: R. Pickering

Question: In the light of the fact that programmes like JSF will have a huge amount of FOD testing, is there a more cost effective way to do FOD testing than ballistic impact?

Answer: Based on the results of the testing shown, techniques other than ballistic are not recommended due to differences in the imposed residual stress states.

Discussor's name: G. Harrison

Comment. Although the 30°impacted specimens showed more scatter, they are more representative of the most severe damage seen in service. Under such conditions airfoil thickness becomes important especially with regard to the magnitude of the damaging tensile stresses. Under such impact conditions adiabatic shear and localised cracking can be observed.

Answer: I agree with the comment. The off angle (30°) testing on airfoil specimens were more closely representative of realistic FOD. The testing on flat plate specimens was an approach to isolate more simplistically, any specific events.